

The split cube in a cage: bulk negative-index material for infrared applications

This article has been downloaded from IOPscience. Please scroll down to see the full text article.

2009 J. Opt. A: Pure Appl. Opt. 11 114010

(<http://iopscience.iop.org/1464-4258/11/11/114010>)

View [the table of contents for this issue](#), or go to the [journal homepage](#) for more

Download details:

IP Address: 192.38.67.112

The article was downloaded on 28/06/2012 at 09:27

Please note that [terms and conditions apply](#).

The split cube in a cage: bulk negative-index material for infrared applications

A Andryieuski¹, C Menzel², C Rockstuhl², R Malureanu¹ and A V Lavrinenko¹

¹ DTU Fotonik—Department of Photonics Engineering, Technical University of Denmark, Ørstedsskolevej 343, DK-2800 Kongens Lyngby, Denmark

² Institute of Condensed Matter Theory and Solid State Optics, Friedrich-Schiller-Universität Jena, Max-Wien-Platz 1, D-07743 Jena, Germany

E-mail: andra@fotonik.dtu.dk

Received 10 June 2009, accepted for publication 4 August 2009

Published 16 September 2009

Online at stacks.iop.org/JOptA/11/114010

Abstract

We propose the split cube in a cage (SCiC) design for application in producing a bulk metamaterial. Applying realistic material data for thin silver films, we observe an immediate convergence of the effective parameters obtained with a number of layers towards the bulk properties. Results are obtained by two different numerical techniques: the Fourier modal method and the finite integrals method, thus ensuring their validity. The SCiC exhibits a refractive index of -0.6 for frequencies close to the telecommunication bands. The fast convergence of effective parameters allows consideration of the SCiC as a bulk (effectively homogeneous) negative-index metamaterial even for a single layer. The bulk-like nature together with the cubic symmetry of the unit cell make the SCiC a promising candidate for potential applications at telecommunication frequencies.

Keywords: negative-index material, bulk metamaterial, 3D metamaterial, effective homogeneity

1. Introduction

There is a strong desire nowadays to obtain negative-index materials (NIMs) [1, 2] operating at optical and infrared frequencies. A series of solutions have been published recently aiming for different applications: superlenses [3], cloaking [4], nanocoupling [5] etc. The most conventional examples of NIMs nowadays are the combination of a wire medium [6] with split-ring resonators (SRRs) [7], cut-wire pairs [8] and a fishnet structure [9]. In the literature one may find a detailed overview of the optical properties [10–14] and fabrication [15–18] of NIMs.

New requirements for metamaterials (MTMs) are on the agenda now: for enhanced effective properties. Most of the proposed NIMs are based on a planar concept. This results in high anisotropy and strong polarization dependence that is undesirable for their application, for example, for obtaining superlenses. To achieve isotropic response, meta-atoms can be either arranged in a cubic structure [19] or dispersed

randomly [20]. Various approaches have been elaborated for constructing an isotropic NIM: SRR-based unit cells [21], Mie resonances of dielectric spheres [22–24] and the ‘nanocircuit paradigm’ [25] for negative permittivity and permeability in the visible. Unfortunately, in most cases the designs for NIMs operating at optical frequencies require dielectric properties of materials which do not exist in nature.

Along the path to obtaining an isotropic NIM the first crucial step is dealing with the requirement for a polarization insensitive NIM. This implies that there is no preference for the orientation of the electric vector relative to the unit cell arrangement, for observing the negative index at normal incidence. Recently we have introduced our generic approach, possessing cubic symmetry [26]. The idea of the nested structures approach is to embed the part exhibiting negative $\text{Re}(\mu)$ into the part providing negative $\text{Re}(\epsilon)$ keeping the total symmetry (cubic) the same. We also proposed the split cube in a cage (SCiC) design. To analyze its response we used material data for bulk silver. In this paper we present the effective

properties of the SCiC with more realistic damping [27] (in the metallic nanostructures the collision frequency increases when the mean free path for electrons is comparable to the film thickness). The SCiC has a simple cubic lattice and its unit cell respects all the symmetry relations in order to be qualified for presenting an effective isotropic structure [19]. In addition, the SCiC's topology allows describing it just in terms of permeability and permittivity, neglecting terms responsible for bianisotropy [19].

It is quite common for metamaterials for the effective properties of a few layers to not be the same as those of many layers. In some scenarios the effective refractive index may even change its sign [28] depending on the number of layers that are used to build up the MTM. We prove here that the SCiC is really a bulk metamaterial (i.e. effectively homogeneous). To call MTM a bulk material we require fast convergence of the effective parameters with increasing number of unit cells (layers) in the direction of propagation towards bulk properties. These bulk properties are accessed by computing the dispersion relation of the eigenmodes propagating in the MTM. They are strictly defined only for the bulk medium. The identity of the effective index as retrieved from the dispersion relation to the index as retrieved from reflection/transmission of a finite structure will prove that the effective parameter concept is valid starting from a single SCiC layer.

The paper is organized as follows. After introducing the parametric space of the design (section 2) we briefly analyze its constitutive parts and proceed to retrieve the effective properties of the samples with different thicknesses in section 3. Effective properties were checked by two numerical methods, which are intrinsically different, thus proving our claims of observing effective bulk properties. The physical mechanisms of the SCiC operation are discussed in detail. Discussion of results and the conclusion end the paper.

2. Methodology

2.1. Design

A negative-index material typically consists of two parts, one of them providing a negative electric response and the other one a negative magnetic response. The nested structures approach [26] proposes inserting a magnetic resonating structure with $\text{Re}(\mu) < 0$ inside a modified grid-like structure that has $\text{Re}(\epsilon) < 0$.

The SCiC unit cell consists of two silver parts embedded in silica (refractive index $n = 1.5$): the inner split cube (SCube) (figure 1(A)) and the outer cage (figure 1(B)). The former acts like a SRR providing negative permeability, whereas the later mimics a 3D wire medium and acts like a diluted metal. For numerical simulations, silver is regarded as a Drude metal with plasma frequency $\omega_p = 1.37 \times 10^{16} \text{ rad s}^{-1}$ and collision frequency $\nu_c = 8.50 \times 10^{13} \text{ s}^{-1}$ [27].

The SCube is a hollow cube with edge length 160 nm and wall thickness 20 nm. Symmetrical horizontal and vertical slits of width 4 nm are carved through the centers of the facets (figure 1(A)).

The cage consists of $a = 250 \text{ nm}$ long square wires of width 20 nm equidistantly placed at the periphery of the unit

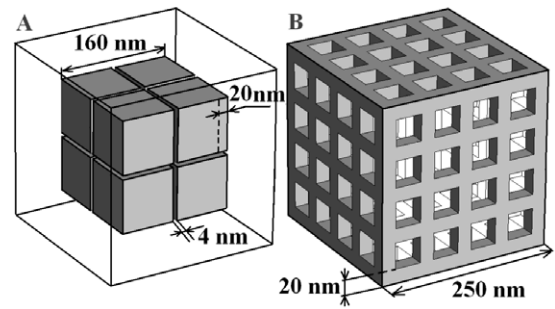


Figure 1. Two constitutive parts of the split cube in a cage unit cell design: (A) split cube, (B) cage.

cell, five wires per cube edge. The cubic structure has lattice constant $a = 250 \text{ nm}$, so the cages from the neighboring unit cells are connected. The cage's appearance recalls a design proposed in [29]; however, their physical properties are considerably different. In the structure from [29] the perforated plates of the neighboring unit cells are not connected. As a result such structure does not provide negative $\text{Re}(\epsilon)$ but instead exhibits very high positive ϵ . So it is operating not like a diluted metal, but rather like a dielectric material with a high permittivity.

The low wavelength limit below which a MTM may be regarded as homogeneous is $\lambda_{\text{lim}} = 4an$ [30], with a the lattice constant and n the refractive index of the embedding dielectric. For the defined parameters of the SCiC the homogeneity limit is $1.5 \mu\text{m}$ which corresponds to the frequency 200 THz. However, close to the resonances the wavelength can be effectively smaller, so it is always worth checking the correctness of the effective parameter model in the frequency range of interest.

2.2. Simulation and effective parameter retrieval

To simulate the transmission/reflection spectra for the metamaterial slab and dispersion diagram for the SCiC we use two numerical methods that are different in principle. Reflection/transmission spectra were calculated with the CST Microwave Studio software (Computer Simulation Technology GmbH, Darmstadt, Germany), which implements the finite integrals technique in the frequency domain, and with a 'homemade' code based on the Fourier modal method (FMM) [31]. The effective parameters were retrieved from the reflection/transmission spectra under normal incidence by relying on the procedure proposed by Smith *et al* [32]. The data obtained in simulations by both methods were thoroughly compared. The results were on a qualitative level the same. Quantitatively, there were some minor deviations. A small steady shift in resonant frequency (less than 6%) was observed due to the usage of essentially different numerical techniques. In addition, time domain simulations of the electromagnetic field maps were done using the CST Microwave Studio. Band dispersion analysis was done by the FMM taking into account the frequency dispersion of the metal parts in the unit cell. To avoid any misinterpretations, we decided to show the results for the SCiC obtained by one method only (the FMM).

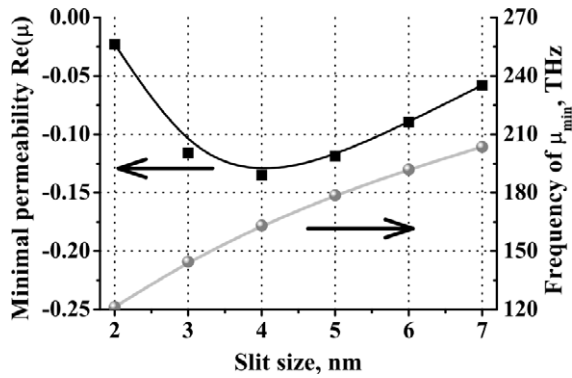


Figure 2. Dependence of the minimal value of the SCube permeability and the resonance frequency on the slit size.

3. Results

3.1. Constitutive parts

The cage consists of long wires, so it can be regarded as an analogue of a 3D wire medium. The properties of the cage resemble those of a plasma [6]. The cage shows high reflectivity (almost 1) and low transmissivity (less than 0.01) even for a single layer. Its effective permittivity has a Drude-like dependence similar to that of bulk silver, but approximately one order in magnitude smaller. Increasing the number of wires per edge and simultaneously decreasing the wire width keeping the same amount of metal pushes the permittivity to be ‘more negative’, i.e. higher in the absolute value. For obtaining large magnitudes of negative dielectric constant ϵ it is preferable to make a lot of thin wires. At the same time, such an approach poses problems both in simulations, since a large number of fine details require large computational resources, and eventually in fabrication, since multiple processing steps are required. Hence, we consider five wires per edge as a good compromise.

Not surprisingly, the effective permittivity and permeability of the cage with wires of width 20 nm show fast convergence with the number of layers. The real part of the effective magnetic permeability is less than 1.0, indicating a pronounced diamagnetic response similar to the diamagnetic response of an inductively loaded loop [33].

The part which brings about a negative magnetic response in our structure is the split cube. The proposed split cube magnetic meta-atom may be regarded as a 3D generalization of a multiple-gap SRR [34]. Magnetic resonance frequency and strength are often explained in terms of an *RLC*-circuit [35]. In the SCube the slits carved in the centers of the cube’s facets play the role of capacitors, while the rest of the SCube plays the role of the inductors and resistors. The size of the slits greatly affects the resonance frequency because of the capacitance associated with it. The variation of the slit from 2 to 7 nm leads to the pronounced resonance frequency shift from 121 to 203 THz (figure 2). The minimum of the effective permeability, -0.13 , corresponds to the slit size 4 nm, so we chose this value in all subsequent simulations.

The existence of the optimal value for the slit width can be explained by the interplay of the growth of the resonance

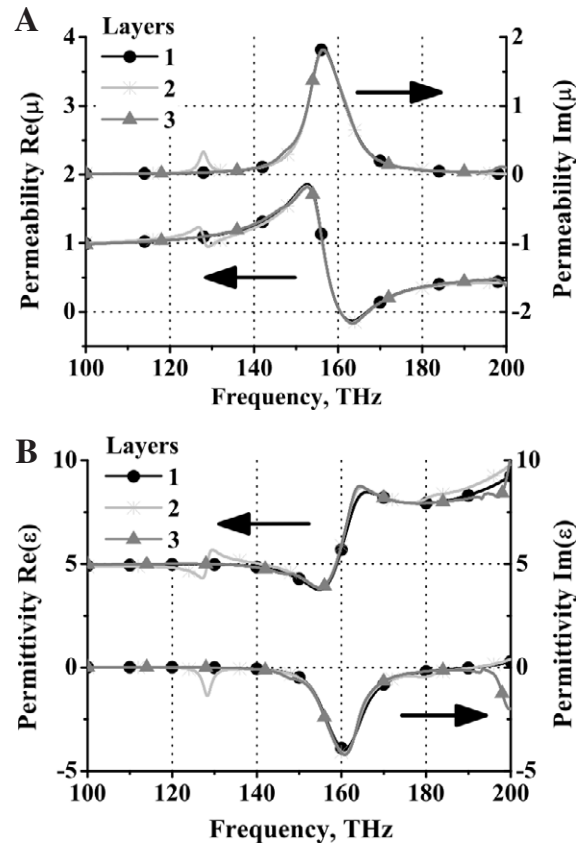


Figure 3. Retrieved effective permeability (A) and permittivity (B) of one (black circles), two (light gray asterisks) and three (gray triangles) layers of the SCube structure. The color and symbol convention will be preserved in all the subsequent figures.

strength with the increase of the capacitance and the increasing role of the direct field tunneling through the very thin dielectric gap.

A decisive effect of such parameters as the SCube’s length and wall thickness is that they determine the area of the circuit, and its inductance and resistance. Thickness also influences its capacitance. Higher values for the resonance strength correspond to a larger SCube length and smaller thickness, but as trade-off the resonance occurs at lower frequency. On one hand the larger length and, consequently, the larger area mean easier magnetic dipole excitation. On the other hand the SCube should not be too close to the cage in order to prevent strong interaction between them. The consequence of this interaction is a shift in the effective plasma frequency.

As regards the influence of the thickness we should remember that the SCube is not exactly a SRR, and by increasing the thickness of the side walls we also change the thickness of the front (and back) walls, which means less penetration of incident waves into the structure. Small thickness allows these waves to penetrate more, but leads in turn to resistance increase, and thus eventually the negative character of $\text{Re}(\mu)$ is lost. We decided that a reasonable compromise is provided by length 160 nm and thickness 20 nm. The permeability (figure 3(A)) and permittivity (figure 3(B)) restored for a SCube several layers thick show good convergence.

In the imaginary part of the permittivity there is a region of negative values that is occasionally associated with a gain medium. In fact, there is no gain in the SCiC structure and a decision on whether a gain occurs cannot be drawn from the permittivity alone. The quantity that plays a decisive role is the imaginary part of the propagation constant which has to be always positive to ensure an exponentially decaying wave. This holds for all our structures. The encountering of a negative imaginary part of the permittivity is the so called ‘anti-resonance’ phenomenon, which has been widely discussed in the literature; see for example discussions in [36–38].

3.2. The split cube in a cage

Aiming at a negative refractive index, we insert the split cube into the center of the cage. Transmission through one layer of the SCiC exhibits two peaks, which are better seen as dips in the reflectivity spectra (figure 4(B)). The first peak around 178 THz shows low transmissivity ($T = 0.05$), but high absorption, $A = 1 - T - R = 0.35$. This peak remains in the spectra with increasing number of layers. This is the frequency region of the magnetic resonance of the SCube and the transmissivity peak corresponds to a region of negative refractive index.

The remarkable property of our design is that the effective parameters (n, ϵ, μ ; figure 5) retrieved from the reflection/transmission simulations converge extremely fast with the number of layers. Within a fairly sufficient approximation we might say that they do not change at all. The effective refractive index $\text{Re}(n)$ is negative in the range from $f_1 = 166$ THz to $f_2 = 183$ THz, reaching the minimum value of -0.62 at 175 THz (figure 5(A)). The maximum figure of merit $\text{FOM} = -\text{Re}(n)/\text{Im}(n)$ is 0.33 at 176 THz. The SCiC suffers a lot from optical losses (figure 5(A)). And this is not surprising as the SCiC is a singly negative material. There is no negative permeability (figure 5(B)), in contrast with the case for the SCube itself (figure 3(A)), and at the same time its permittivity is Drude-like (figure 5(C)). We conclude that the reduction in the SCiC’s magnetic response comes from the interaction between the cage and the SCube structures.

To confirm that the SCiC metamaterial acts like a bulk material, we calculated its dispersion diagram for waves propagating in a Γ -X direction of the simple cubic lattice, imposing periodic boundary conditions and thus mimicking the infinite lattice. The real part of the propagation constant as a function of the frequency for the lowest Bloch mode is compared with the effective wavenumber $k = k_0 n$ obtained from the reflection/transmission simulations for the finite number of layers (figure 6(A)). The graphs completely coincide with each other, thus confirming the thesis that the effective propagation constant is the same for the SCiCs consisting of from one to an infinite number of layers. We would like to note that the lowest mode is doubly degenerate due to polarization independence of the SCiC unit cell.

4. Discussion

Usually effective wave parameters of MTMs are modified depending on the number of layers, but experience convergence

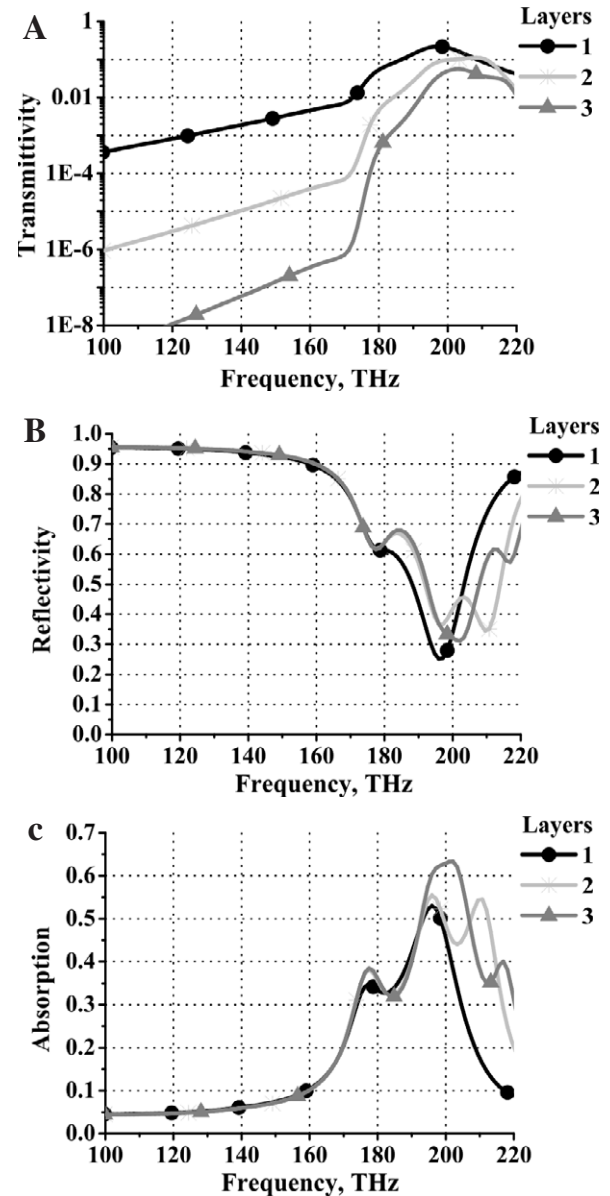


Figure 4. Transmittivity (A), reflectivity (B) and absorption (C) spectra of one, two and three layers of the SCiC structure.

with increasing thickness [28]. However, this also pushes the effective parameter concept close to the boundaries of its validity. In our case the effective parameter convergence with the number of layers is impressive. It confirms that we might regard a split cube in a cage as a bulk metamaterial starting from a single(!) layer. Similar fast convergence has been recently reported for meander-like wire metamaterials [39]. Unfortunately, the latter design allows only fixed preferable direction of the electric field.

Poor convergence of the effective parameters can be also explained with the non-negligible impact of higher order Bloch modes. To analyze our structure using such an approach we plot imaginary parts of the wavevector of several Bloch modes extracted with the help of the FMM (figure 6(B)). The imaginary part of the k versus ω diagram characterizes losses of the optical modes. The attenuation constants (losses)

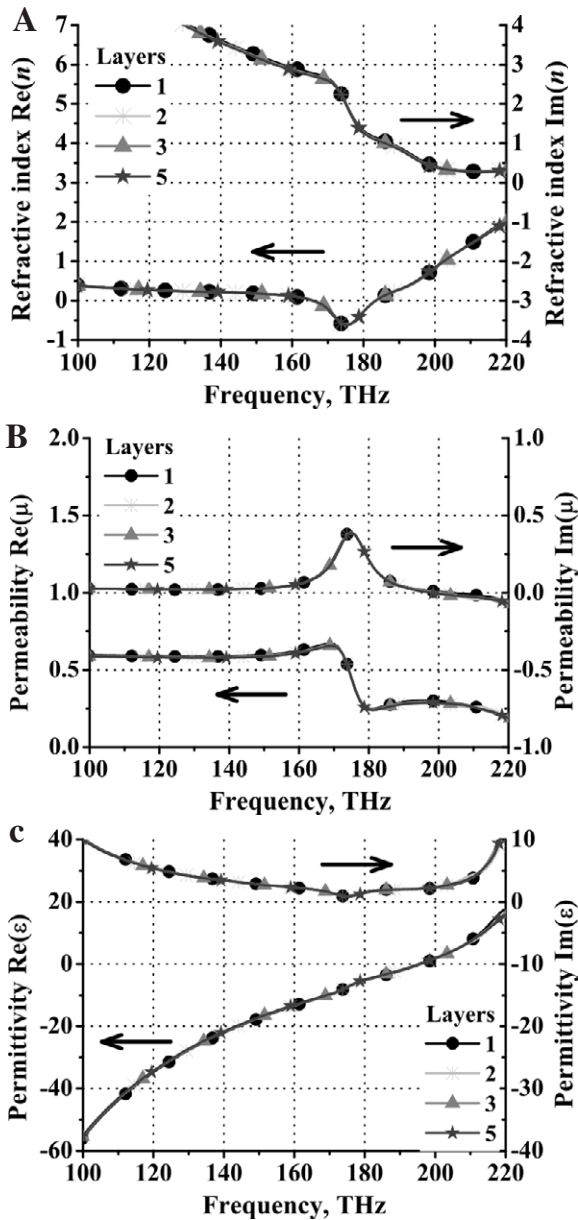


Figure 5. Effective refractive index (A), permeability (B) and permittivity (C) spectrum for one, two, three and five (dark gray stars) layers of the SCiC structure.

are comparable for the two modes only. For example, at frequency 173 THz the damping for mode No. 3 is only $0.5\pi/a$ higher than the damping of the lowest doubly degenerate mode. However, the higher order mode does not couple at all with the incident plane wave since it has an antisymmetric field distribution, whereas the exciting plane wave only provides a symmetric field distribution [40]. Therefore, it cannot affect the picture of the light propagation in the frequency interval of interest. Otherwise, interaction of two excited modes would lead to slow convergence of the effective parameters that is definitely not observed in our case. The next higher order modes which possess a symmetric field distribution are much more strongly damped as compared to the lowest order mode and will therefore not contribute to the light transport through

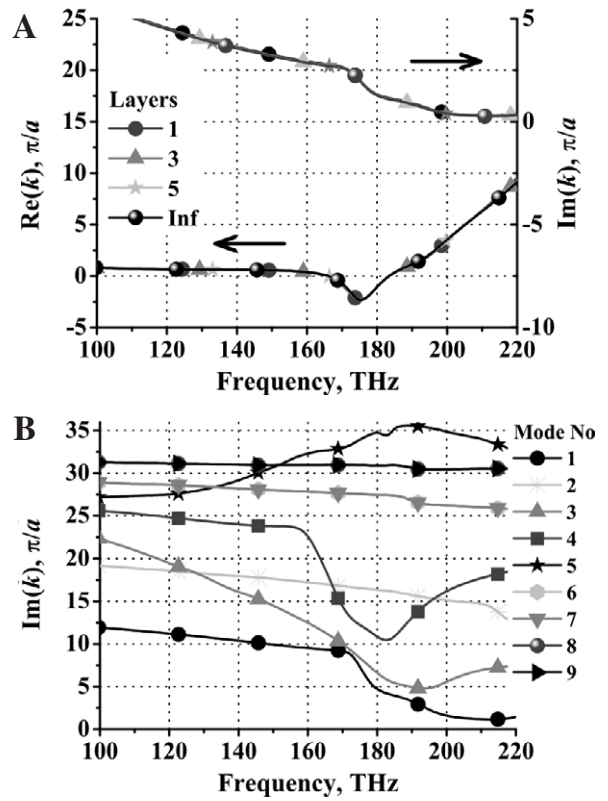


Figure 6. Propagation constant for one, three, five and an infinite number of layers of the SCiC (A). Damping for different Bloch modes—Nos 1–9 (B).

the structure. This possibility of exciting only a single mode inside the metamaterial ultimately causes the extraordinary agreement between the effective properties as retrieved for a single layer and those retrieved from the dispersion relation.

The interesting question is that of the nature of the transmission peaks. We identify the first peak at 178 THz as a consequence of NIM behavior occurring in the SCiC unit cell. To prove this we perform time domain simulations; see the mapping of the electric field in figure 7(A). These clearly show the excitation of a loop current (i.e. a magnetic dipole) in the SCube part. As in a 2D SRR [7] the electric field in the SCube’s slits is much enhanced in comparison with that of the incident wave.

The second peak, which is around 197 THz in the case of one layer, has the highest transmission, around 0.22. The time domain simulation (see the mapping of the electric field in figure 7(B)) reveals the excitation of an electric dipole in the SCube at this frequency. The electric field below and above the SCube is much stronger than the electric field of the incident wave. The field inside the SCube is very weak, as the SCube effectively screens it.

We explain the appearance of this transmission peak as stemming from the introduction of a defect in a conventional Fabry–Perot resonator. Indeed, the cage itself can be regarded as a Fabry–Perot resonator (two reflecting mirrors on either side of a dielectric slab). However, its first transmission maximum according to its spatial parameters is anticipated to be at around 400 THz. Therefore, a poor transmission around

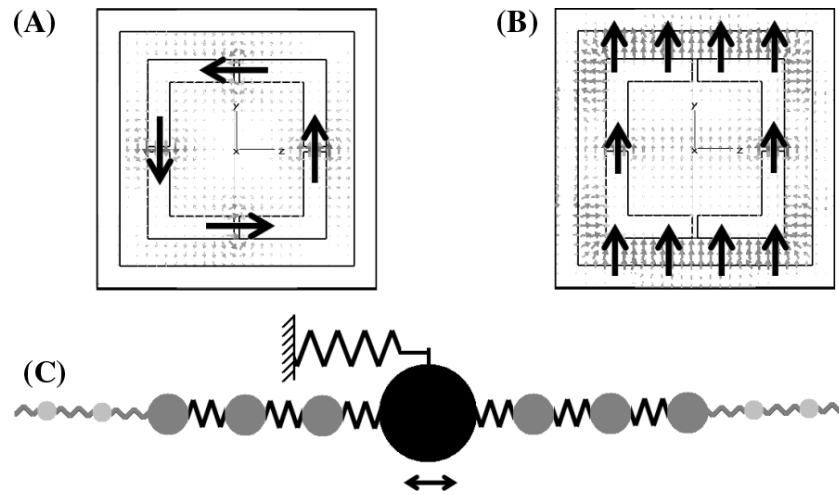


Figure 7. Electric field distribution inside the unit cell of the SCiC at magnetic resonance frequency 178 THz (A) and at frequency 197 THz corresponding to the maximum of transmission (B). Mechanical analogy of the Fabry–Perot resonator with resonant inclusion (C).

frequency 200 THz is expected. If we place inside the Fabry–Perot cavity a resonant inclusion with an eigenfrequency somewhere around 200 THz, the minimum in transmission will experience significant growth that has a resonant character. This can be easily understood by applying a mechanical model where a massive resonant inclusion rules the properties of the mechanical analogue of the Fabry–Perot resonator—the springs–balls system (figure 7(C)). For several SCiC layers the Fabry–Perot peak splits corresponding to the number of layers (figure 4(C)) as a consequence of the coupling between neighboring SCubes.

The slit size influences the performance of the magnetic resonance. Changing the slits from 4 to 5 nm leads to the non-convergence of the effective parameters that took place in [26]. The reason for such unfavorable behavior is that the frequency of the magnetic resonance is shifted higher (figure 2) and becomes too close to the eigenfrequency of the dipole-like resonance of the SCube. Increasing the number of SCiC layers, we change the eigenfrequency of the dipole resonance, due to the coupling between the SCubes of different layers. SCubes can be regarded as *LC*-circuits, and coupling of the *LC*-circuits leads to decrease of the lowest eigenfrequency. This decreases the effective plasma frequency and the effective properties of the SCiC change, so it loses the negative refractive index. This also means that we cannot use the Fabry–Perot resonator to enhance transmission in the $\text{Re}(n) < 0$ region.

Our analysis clearly indicates high sensitivity of the MTM design to fabrication tolerances. Even such small changes in slit sizes as 1 nm lead to abrupt transformation of the SCiC refractive index behavior. Neither metal–organic vapor phase deposition [16] nor electroless deposition [41] are currently capable of providing metallic nanostructures within the tolerance range below 1 nm. To be fabricated, the SCiC design needs considerable simplification. However, we are also optimistic about the progress in fabrication techniques.

5. Conclusions

In this paper we analyzed in detail the physical behavior and the effective parameters of the split cube in a cage negative-index metamaterial and its constitutive elements. The cage behaves according to the Drude model, giving negative permittivity $\text{Re}(\epsilon)$ over a broad range of frequencies and a diamagnetic response. The split cube is responsible for the negative permeability $\text{Re}(\mu)$. Its magnetic resonance strength and frequency strongly depend on the geometrical sizes of SCube.

The transmission spectrum for one layer of the SCiC exposes two pronounced peaks. One is identified as being due to the negative refractive index and another can be explained with the model of a Fabry–Perot resonator with a resonant inclusion. It was shown that the Fabry–Perot effect cannot be used to enhance the transmissivity of the peak for the negative refractive index. The minimal negative $\text{Re}(n)$ for one layer of the SCiC is -0.62 . The effective parameters show extremely fast convergence with the number of layers.

The SCiC structure has a potential for application as a 3D polarization insensitive bulky negative-index material. The optical isotropy should be checked by thorough analysis that is currently beyond the scope of this paper. The losses and fabrication implications are among the main problems. We believe that both issues can be addressed by further structural optimizations.

Acknowledgments

The authors gratefully acknowledge partial support from the Danish Research Council for Technology and Production Sciences via the NIMbus project, from COST Action MP0702: Towards Functional Sub-Wavelength Photonic Structure, from the German Federal Ministry of Education and Research (Metamat) as well as from the State of Thuringia within the Pro-Excellence program (MeMa).

References

- [1] Veselago V G 1968 *Sov. Phys.—Usp.* **10** 509
- [2] Smith D R, Padilla W J, Vier D C, Nemat-Nasser S C and Schultz S 2000 *Phys. Rev. Lett.* **84** 4184
- [3] Pendry J B 2000 *Phys. Rev. Lett.* **85** 3966
- [4] Schurig D, Mock J J, Justice B J, Cummer S A, Pendry J B, Starr A F and Smith D R 2006 *Science* **314** 977
- [5] Degiron A, Smith D R, Mock J J, Justice B J and Gollub J 2007 *Appl. Phys. A* **87** 321
- [6] Rotman W 1962 *IRE Trans. Antennas Propag.* **10** 82
- [7] Pendry J B, Holden A J, Robbins D J and Stewart W J 1999 *IEEE Trans. Microw. Theory Tech.* **47** 2075
- [8] Shalaev V M, Cai W, Chettiar U K, Yuan H K, Sarychev A K, Drachev V P and Kildishev A V 2005 *Opt. Lett.* **30** 3356
- [9] Zhang S, Fan W, Malloy K J, Brueck S R J, Panoiu N C and Osgood R M 2005 *Opt. Express* **13** 4922
- [10] Pendry J B 2009 *Contemp. Phys.* **50** 363
- [11] Shalaev V M 2007 *Nat. Photon.* **1** 41
- [12] Busch K, Freymann G, Linden S, Mingaleev S F, Tkeshelashvili L and Wegener M 2007 *Phys. Rep.* **444** 101
- [13] Padilla W J, Basov D N and Smith D R 2006 *Mater. Today* **9** 28
- [14] Soukoulis K M, Kafesaki M and Economou E N 2006 *Adv. Mater.* **18** 1941
- [15] Boltasseva A and Shalaev V M 2008 *Metamaterials* **2** 1
- [16] Rill M S, Plet C, Thiel M, Staude I, Freymann G, Linden S and Wegener M 2008 *Nat. Mater.* **7** 543
- [17] Valentine J, Zhang S, Zentgraf T, Ulin-Avila E, Genov D A, Bartal G and Zhang X 2008 *Nature* **455** 376
- [18] Lezec H J, Dionne J A and Atwater H A 2007 *Science* **316** 430
- [19] Baena J, Jelinek L and Marques R 2007 *Phys. Rev. B* **76** 245115
- [20] Born M and Wolf E 1999 *Principles of Optics* (Cambridge: Cambridge University Press)
- [21] Koschny T, Zhang L and Soukoulis C M 2005 *Phys. Rev. B* **71** 121103
- [22] Yannopoulos V and Moroz A 2005 *J. Phys.: Condens. Matter* **17** 3717
- [23] Vendik I, Vendik O and Odit M 2006 *Microw. Opt. Technol. Lett.* **48** 2553
- [24] Kussow A, Akyurtlu A and Angkawisittpan N 2008 *Phys. Status Solidi b* **245** 992
- [25] Engheta N 2007 *Science* **317** 1698
- [26] Andryieuski A, Malureanu R and Lavrinenko A 2009 *J. Eur. Opt. Soc.: Rapid Publ.* **4** 09003
- [27] Dolling G, Enkrich C and Wegener M 2006 *Opt. Lett.* **31** 1800
- [28] Rockstuhl C, Paul T, Lederer F, Pertsch T, Zentgraf T, Meyrath T P and Giessen H 2008 *Phys. Rev. B* **77** 035126
- [29] Shin J, Shen J T and Fan S 2009 *Phys. Rev. Lett.* **102** 093903
- [30] Caloz C and Itoh T 2006 *Electromagnetic Metamaterials: Transmission Line Theory and Microwave Applications* (Hoboken, NJ: Wiley-Interscience)
- [31] Li L 1997 *J. Opt. Soc. Am. A* **14** 2758
- [32] Smith D R, Schultz S, Markos P and Soukoulis C M 2002 *Phys. Rev. B* **65** 195104
- [33] Economou E, Koschny T and Soukoulis C M 2008 *Phys. Rev. B* **78** 92401
- [34] Penciu R, Aydin K, Kafesaki M, Koschny T, Ozbay E, Economou E and Soukoulis C M 2008 *Opt. Express* **16** 18131
- [35] Tretyakov S 2007 *Metamaterials* **1** 40
- [36] Koschny T, Markos P, Smith D R and Soukoulis C M 2003 *Phys. Rev. E* **68** 65602
- [37] Depine R A and Lakhtakia A 2004 *Phys. Rev. E* **70** 048601
- [38] Efros A L 2004 *Phys. Rev. E* **70** 048602
- [39] Güney D Ö, Koschny T, Kafesaki M and Soukoulis C M 2009 *Opt. Lett.* **34** 506
- [40] Rockstuhl C, Menzel C, Paul T, Pertsch T and Lederer F 2008 *Phys. Rev. B* **78** 155102
- [41] Kuebler S M, Tal A and Cheng Y S 2008 *Proc. SPIE* **6901** 69010Z